Rapid, Selective Heavy Metal Removal from Water by a Metal–Organic Framework/Polydopamine Composite

Daniel T. Sun,[†] Li Peng,[†] Washington S. Reeder,[†,‡] Seyed Mohamad Moosavi,[†] Davide Tiana,[†] David K. Britt,[§] Emad Oveisi,[∥] and Wendy L. Queen*,[†]

[†]Institute of Chemical Sciences and Engineering, École Polytechnique Fédérale de Lausanne (EPFL), CH-1051 Sion, Switzerland

[‡]Department of Chemical and Biomolecular Engineering, University of California, Berkeley, Berkeley, California 94720, United States

[§]The Molecular Foundry, Materials Sciences Division, Lawrence Berkeley National Laboratory, Berkeley, California 94720, United States

[∥]Interdisciplinary Center for Electron Microscopy, École Polytechnique Fédérale de Lausanne (EPFL), CH-1015 Lausanne, Switzerland

S *Supporting Information*

ABSTRACT: Drinking water contamination with heavy metals, particularly lead, is a persistent problem worldwide with grave public health consequences. Existing purification methods often cannot address this problem quickly and economically. Here we report a cheap, water stable metal–organic framework/polymer composite, Fe-BTC/PDA, that exhibits rapid, selective removal of large quantities of heavy metals, such as Pb^{2+} and Hg^{2+}, from real world water samples. In this work, Fe-BTC is treated with dopamine, which undergoes a spontaneous polymerization to polydopamine (PDA) within its pores via the Fe^{3+} open metal sites. The PDA, pinned on the internal MOF surface, gains extrinsic porosity, resulting in a composite that binds up to 1634 mg of Hg^{2+} and 394 mg of Pb^{2+} per gram of composite and removes more than 99.8% of these ions from a 1 ppm solution, yielding drinkable levels in seconds. Further, the composite properties are well-maintained in river and seawater samples spiked with only trace amounts of lead, illustrating unprecedented selectivity. Remarkably, no significant uptake of competing metal ions is observed even when interferents, such as Na^+, are present at concentrations up to 14 000 times that of Pb^{2+}. The material is further shown to be resistant to fouling when tested in high concentrations of common organic interferents, like humic acid, and is fully regenerable over many cycles.
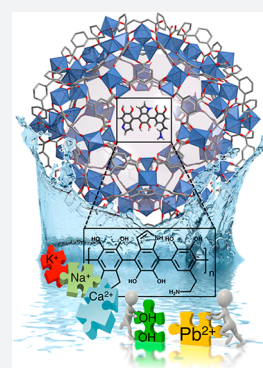
INTRODUCTION

With an estimated 1 billion people without access to clean drinking water and 2 million casualties per year, water contamination is currently one of the world's leading causes of death.[1] This problem is only expected to worsen as the World Health Organization (WHO) estimates that climate change will limit access to clean water for as much as half of the world's population,[2] and a recent United Nations report projects that the world could face a 40% water shortage in as few as 15 years.[3] A surge in energy production and an exponential increase in heavy metal use in industrial processes have caused a rise in human exposure to toxic heavy metals in recent decades.[4] The high toxicity and prevalence of cadmium, chromium, lead, arsenic, and mercury put them among the greatest concern. These metals, which play no role in human homeostasis, induce multiple organ damage, cause birth defects, and are classified carcinogens.[4] To maintain environmental and human well-being, it is imperative that we find new solutions for the cheap, energy efficient remediation of trace contaminants from water.[5,6]

The high abundance of lead has steered its incorporation into a number of products, such as pigments, paints, ceramic glazes, jewelry, toys, etc. Further, municipal drinking water in many countries is still delivered through lead pipes or pipes joined with lead solder. Consequently, aging infrastructure makes lead one of the most prominent metals seen in human exposure cases. Recently, the media has described extensive lead exposure in several developed countries shedding light on our inability to rapidly clean contaminated water on large scales. Virginia Tech researchers uncovered extensive lead contamination in Flint, Michigan,[7] and in December of 2016 a study by Reuters reported more than 3000 areas in the US with poisoning rates twice that of Flint.[8] Unfortunately, exposure is even worse in underdeveloped countries where a lack of resources and awareness limits the use of expensive industrial wastewater treatment processes.[9,10] Given these problems, the WHO has recently declared lead as 1 of 10 chemicals of major public health concern, necessitating action by Member States to protect the population.[11]

Commercial heavy metal remediation methods, such as chemical precipitation, sorbents, and membranes, have many disadvantages that include high economic and energy cost, low removal efficiency, difficult regeneration and/or fouling, and

the production of large quantities of chemical sludge.[5] As a result, even well documented cases of contamination in developed countries are left without remediation. These inadequacies have sparked our interest in the exploration of inexpensive metal−organic frameworks (MOFs) for water purification. This class of porous materials has quickly moved to the forefront of materials research due to their unprecedented internal surface areas, facile chemical tunability, and extraordinary capability to selectively adsorb large quantities of guest species.[12−14] The potential to deploy MOFs in water purification is related to the ease with which their internal surfaces can be postsynthetically decorated with high densities of strong adsorption sites.[15−17] Further, recent reports show that amorphous polymers with intrinsic porosity can compete in both rate and capacity with benchmark adsorbents for water treatment.[18−20] Therefore, we hypothesize that MOFs could be used to introduce extrinsic porosity to polymers comprised of high densities of metal-scavenging functionality (Figure 1). In this work, a biologically[21] and
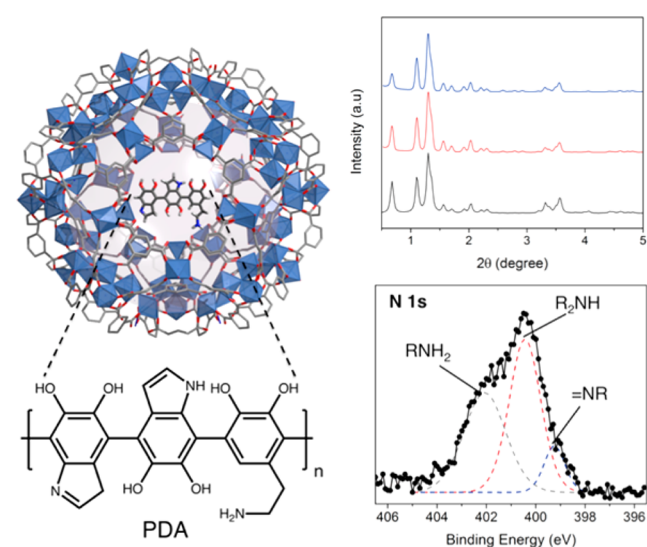

Figure 1. Characterization of Fe-BTC/PDA. (Left) Polyhedral view of a large cage in the Fe-BTC with PDA embedded inside the channels. The purple sphere represents the void space inside of the cage prior to the dopamine addition. (Top) The simulated XRD pattern of Fe-BTC (black) compared to the synchrotron XRD data ($\lambda = 0.50084$ Å) of Fe-BTC (red) and Fe-BTC/PDA-19 (blue). (Bottom) X-ray photo-electron spectroscopy data obtained from the N 1s spectrum of Fe-BTC/PDA-19.

environmentally friendly MOF, Fe-BTC (alternatively known as MIL-100; BTC = 1,3,5-benzenetricarboxylate),[22,23] which features triangular Fe_3O clusters interlinked by BTC^{3-} ligands, is used as a porous template for the anaerobic polymerization of dopamine. Polydopamine (PDA) contains amine and catechol functionalities that not only are capable of scavenging metals but also provide a pathway to adhere the polymer onto the internal MOF surface.[24] The latter inhibits the dispersion of the hydrophilic PDA into water and, hence, facile separation post-water treatment. The resulting composite combines high capacity, selectivity, and a record-breaking removal rate of Pb^{2+} and Hg^{2+} ions, making it a highly promising material for decontamination of drinking water.

RESULTS AND DISCUSSION

Fe-BTC, synthesized using known procedures,[25] possesses empty mesoporous cages of 25 and 29 Å diameter that can be accessed via microporous windows of about 5.5 and 8.6 Å diameter, respectively. The resulting material has a BET surface area of 2324 m^2/g and open metal coordination sites (Figure S2), which can be used to append PDA on the internal MOF surface. Density functional theory (DFT) calculations were utilized to assess the feasibility of PDA binding to Fe^{3+} sites (Figure S10 and Table S2). The calculated relative binding energies indicate that the O and N containing functionalities on the polymer are expected to bind readily to the metal ion, implying that the polymer has a high affinity for the internal MOF surface.

The Fe-BTC/PDA composite is formed by mixing the desolvated MOF with dopamine (see the Methods and Materials Section of the SI). The redox active Fe^{3+} sites[26] are found to promote the anaerobic oxidation of dopamine to form PDA, which causes a color change in the MOF from light orange to dark purple. While the anaerobic oxidation of dopamine via Fe^{3+} has been previously reported, to the best of our knowledge, it has not been carried out in a porous adsorbent.[27] The resulting composite is found to contain a modest loading of PDA, 19 mass % (denoted as Fe-BTC/PDA-19), via combustion analysis (Table S1) and exhibits a BET surface area of 1134 m^2/g, with no apparent loss in crystallinity (Figure 1). Fe-BTC/PDA stability was tested by soaking the material for up to two months in Rhone River water containing 0, 1, and 1000 ppm Pb^{2+}. No leaching of iron was observed per ICP-OES, which shows a concentration less than the detectable limit (<10 ppb). Also, after long-term soaking, there is no apparent trace of PDA found in the water samples via MALDI-TOF-MS experiments (Figure S3). Last, powder X-ray diffraction shows that the structural integrity of the MOF is maintained after the soaking process (Figure S3).

Dopamine polymerization was evident by X-ray photo-electron spectroscopy (XPS). The N 1s region of the spectrum was used to look for primary, secondary, and tertiary amines that are indicative of dopamine, polydopamine and its intermediates, and tautomers of the intermediates.[28] The presence of secondary and tertiary amines, which are not present in dopamine, is evidence for the indole formation, a signature of the polymerization process[28,29] (Figure 1). To give further evidence of the polymerization, the composite was soaked in a 4 M HCl solution as an attempt to partially destroy the porous template, and MALDI-TOF-MS spectra show proof of PDA in solution consisting up to 7 monomeric units (Figure S6). Scanning electron microscopy (SEM) reveals no polymer formation on the crystal facets (Figure S7). In order to test conclusively whether the polymer is distributed throughout the MOF, Fe-BTC/PDA-19 was embedded in an epoxy resin and serially sectioned in 100 nm thick slices using an ultra-microtome. Energy dispersive X-ray spectroscopy (EDX) analysis in a scanning transmission electron microscope (STEM) provided evidence that nitrogen, a signature of the polymer, is indeed located throughout the MOF crystal (Figures 2 and S8). The result was further confirmed by STEM electron energy loss spectroscopy (EELS) (Figure S9).

Attenuated total reflectance infrared (ATR-IR) and Raman spectroscopies were used to provide evidence that the polymer is interacting with open Fe^{3+} sites of the MOF (Figure S11). IR data obtained from PDA nanospheres reveal a peak at ~1506
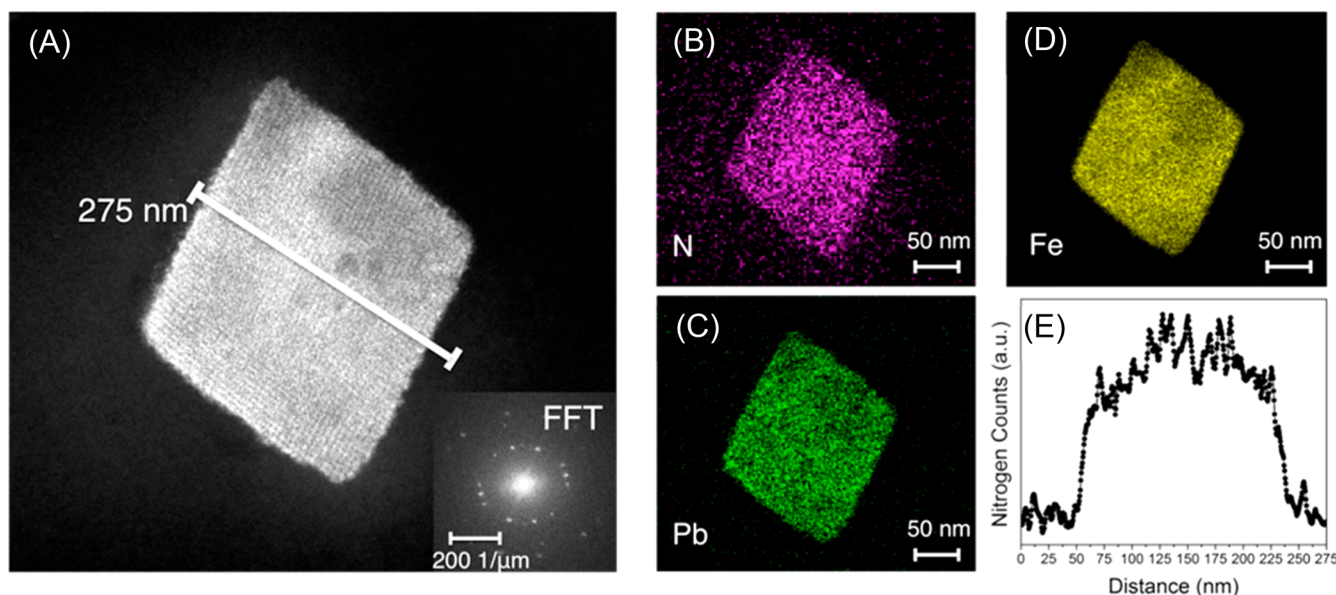
Figure 2. HAADF-STEM images. (A) HAADF-STEM image of a sliced single crystalline of Fe-BTC/PDA-19 and (B−D) the corresponding EDX elemental mapping. (E) STEM-EDX line profile of nitrogen across the region indicated in (A). The line profile is 275 nm long and is integrated over 100 nm. Elemental mapping was done after the composite was soaked in a highly concentrated aqueous solution of Pb^{2+}.

cm^{-1}, which has previously been assigned to an indoline stretching vibration.[30] For Fe-BTC/PDA, this peak is instead split into two bands occurring at ~1482 and ~1556 cm^{-1}, a signature of the formation of an Fe^{3+}−PDA complex.[30,31] Further, when compared to that of Fe-BTC, the Raman spectrum obtained from Fe-BTC/PDA shows a new peak at ~642 cm^{-1}, which previous reports attribute to the stretching modes of Fe^{3+}−catecholate complexes.[32] These results, which also coincide with the aforementioned DFT calculations, indicate that PDA is indeed pinned to the MOF's pore surface through the Fe^{3+} open metal sites.

The accessibility of metal-scavenging catechols within the pores of Fe-BTC/PDA-19, as indicated by a positive Prussian blue test (Figure S12), spurred the exploration of the composite for water treatment. Fe-BTC and Fe-BTC/PDA-19 were soaked in distilled water containing 1 ppm of As^{3+}, Cd^{2+}, Cr^{6+}, Hg^{2+}, or Pb^{2+} (Figures 3 and S13). When compared to Fe-BTC, the composite material significantly enhances the removal of all metals, excluding Cr^{6+}. The removal capacities of As^{3+}, Cd^{2+}, Pb^{2+}, and Hg^{2+} were improved by factors of 6.1, 6.1, 92, and 60, respectively. Additionally, the composite reduced the concentrations of both Pb^{2+} and Hg^{2+} below what is deemed drinkable by the U.S. Environmental Protection Agency (EPA, <15 ppb for Pb^{2+} and <2 ppb for Hg^{2+}).[33] As such, Pb^{2+} and Hg^{2+} extractions were explored for the remainder of the study.

The high performance observed for Fe-BTC/PDA-19 prompted us to determine the effect of polymer loading on the composite's removal capacity. Fe-BTC was loaded with 28, 38, and 42 mass % PDA, resulting in BET surface areas of 757, 488, and 165 m^2/g, respectively (Figure 4 and Table S1). The composites were then used to treat the Rhone River water spiked with 1000 ppm of Hg^{2+} (Figure 4). Removal capacities up to 1634 mg of Hg^{2+} per gram of composite were observed for Fe-BTC/PDA-42, almost 10 times that observed for the unmodified Fe-BTC. For Pb^{2+}, the trend is similar (Figure 4) with removal capacities up to 394 mg per gram of composite, 2.6 times the capacity of the unmodified Fe-BTC. Given the
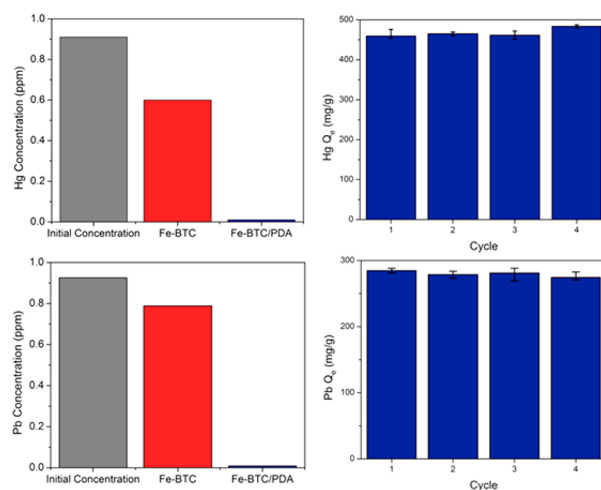

Figure 3. Evaluation of heavy metal remediation. Concentration of (top, left) Hg^{2+} and (bottom, left) Pb^{2+} in distilled water before treatment (grey) and after treatment with Fe-BTC (red) or Fe-BTC/PDA-19 (blue). Uptake capacity of Fe-BTC/PDA-19 after saturation and regeneration cycles using (top, right) Hg^{2+} (with regeneration via ascorbic acid) and (bottom, right) Pb^{2+} (with regeneration via ethylenediaminetetraacetic acid (EDTA)).

enhanced performance of the composite compared to the MOF, we establish that the high density of the heavy metal-scavenging groups on the polymer backbone is the fundamental contributor to the high removal capacities. Several other parameters, such as selectivity, removal rate, and resistance to organic interferents, were also tested for Fe-BTC/PDA-42. Other than higher capacities, this material shows a performance similar to that of Fe-BTC/PDA-19. As such, the composite with the 19 mass % loading is the material discussed throughout this work, because it was the most extensively studied.

Efforts were also made to demonstrate the structural tunability of these novel MOF/polymer composites. For this, many different redox active polymers, containing −OH, −SH,
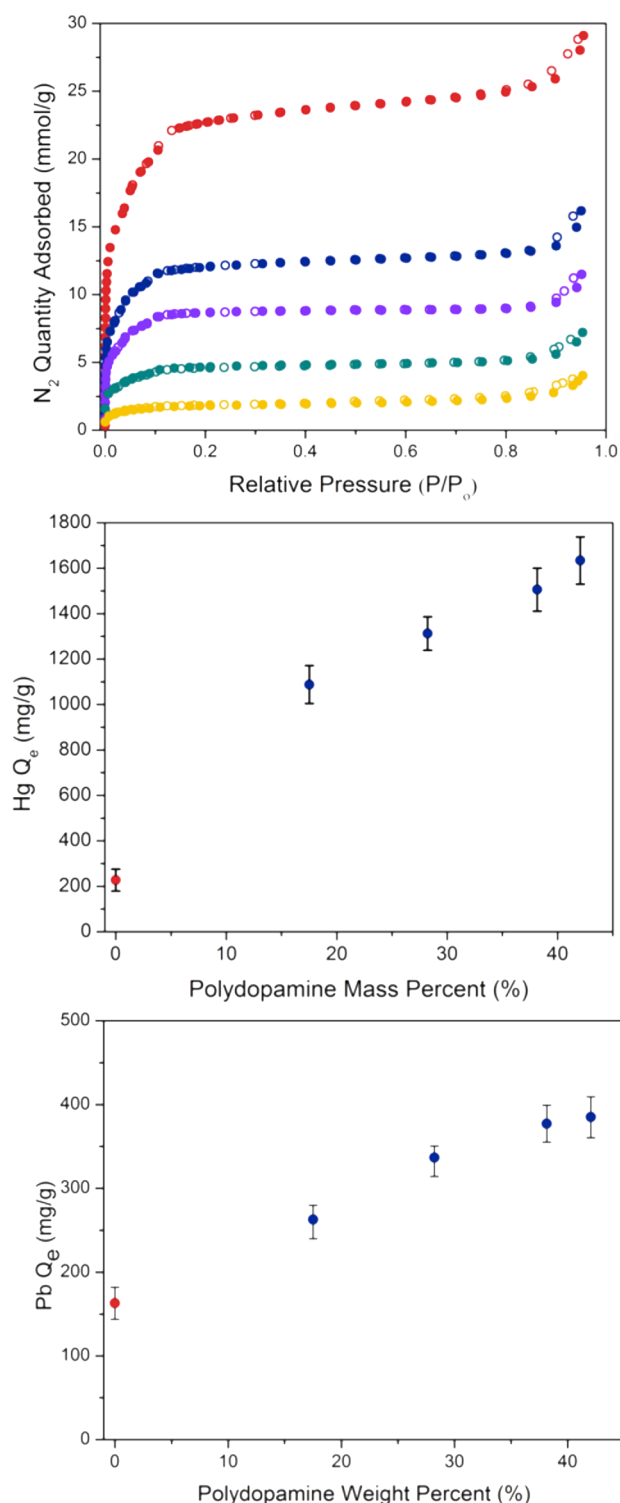
Figure 4. Tuning composite removal capacity. (Top) N_2 adsorption and desorption isotherms for Fe-BTC (red) and several Fe-BTC/PDA composites with 19 (blue), 28 (purple), 38 (green), and 42 (yellow) mass % loading of PDA. The polydopamine loading level provides tunability of the (middle) Hg^{2+} and (bottom) Pb^{2+} removal capacity.

and $-NH_2$ metal-scavenging functionality, were loaded into two MOF templates, including Fe-BTC and Cu-TDPAT[34] (TDPAT = 2,4,6-tris(3,5-dicarboxylphenylamino)-1,3,5-triazine). It can be seen in Figure S24 and Table S6 that these materials readily form, offer fast Pb^{2+} removal rates, and can reduce Pb^{2+} concentrations into the drinkable regime as

observed for Fe-BTC/PDA. Studies intended to demonstrate the use of these materials for the extraction of many other analytes from water and air are currently underway.

To date, there has been an increasing number of studies assessing heavy metal uptake in porous adsorbents.[19,35−38] Throughout the literature, these materials are typically assessed based on a metric known as the calculated distribution coefficient, k_d (Figure S16), which reflects a material's affinity to heavy metals. The consensus is that k_d values higher than 1.0 × 10⁴ are considered to be excellent. The k_d values of Fe-BTC/PDA, 5.5 × 10⁶ and 1.7 × 10⁶ mL/g for Hg^{2+} and Pb^{2+}, respectively, are among the highest reported, particularly for lead (Figure S14). To date, only two studies report materials with lead k_d values that are higher than those of Fe-BTC/PDA, which are a MOF containing Zn paddlewheels (known as $Zn_3L_3(BPE)1.5$, k_d = 2.3 × 10⁶)[39] and a Ni/Cr layered double hydroxide (known as DPA-LDH, k_d = 1.99 × 10⁸).[40] While the k_d is a sufficient measure for a quick initial comparison of materials, it is seen that these materials suffer from long equilibration times (30−60 min)[41,42] and loss in capacity with regeneration.[41] As such, we have provided an extensive comparison of Fe-BTC/PDA to the best performing materials reported to date in Tables S4 and S5. It should be noted that successful implementation of a material in drinking water or wastewater treatment technologies requires a full evaluation of long-term stability, cost-effectiveness, ability to resist clogging from large organic interferents, recyclability, rate of removal, and selectivity over common inorganic interferents. Fe-BTC/PDA is found to perform well in all aforementioned arenas.

Most current adsorbent technologies for water purification, such as activated carbon and functionalized silica, are mesoporous (2−50 nm in size), allowing large organic molecules to diffuse inside. This process often fouls adsorbents, compromising removal capacity.[39,40] Given this, the composite's susceptibility to a common large organic interferent, humic acid, was tested. Fe-BTC/PDA-19 was used to treat solutions with and without humic acid (100 ppm of humic acid and Hg^{2+} and Pb^{2+} concentrations ranging from 200 to 900 ppm) (Figure S17). The composite indeed maintains capacities in the presence of humic acid, likely due to Fe-BTC's unique architecture. The small pore apertures, 5.5 and 8.6 Å, act as gateways into the mesoporous cages, preventing large organic molecules from diffusing into the MOF, while still allowing metal ions to diffuse through.

Since the composite's heavy metal uptake shows a clear pH dependence (Figure S18), the material's reversibility was probed using ascorbic acid and ethylenediaminetetraacetic acid (EDTA). The composite material was first saturated with Pb^{2+} or Hg^{2+} and then treated in the aforementioned additives for 4 h, followed by a subsequent assessment of the composite capacity. For both Pb^{2+} and Hg^{2+}, the composite shows minimal change in capacity over a total of 4 cycles after saturation and regeneration (Figures 3 and S19). While adsorbed Pb^{2+} can be separated completely from the composite, the Hg^{2+} precipitates as solid Hg_2Cl_2, evident by PXRD and XPS (Figures S20 and S21 and Table S3). However, the solid appears to precipitate outside of the framework leaving the regenerated catechols open for continued reduction/precipitation cycles with Hg^{2+}. We surmise that the catechols on the PDA are likely oxidized to the quinone form, as indicated by a negative Prussian blue test (Figure S12), when reducing Hg^{2+} to Hg^+. This observation is consistent with PDA's known ability to reduce several noble metals, such as Au^{3+}, Ag^+, and Pt^{3+}.[29]

The composites' high capacity and reusability provide an extended lifetime that is needed for long-term use in water purification applications.

The metal ion extraction rates of Fe-BTC and Fe-BTC/PDA-19 were determined from distilled water samples spiked with 1000 ppb of Pb^{2+} and Hg^{2+}. We observed that unmodified Fe-BTC reaches a maximum of 18% heavy metal removal (Figure 5) within a minute. Remarkably, when the solutions
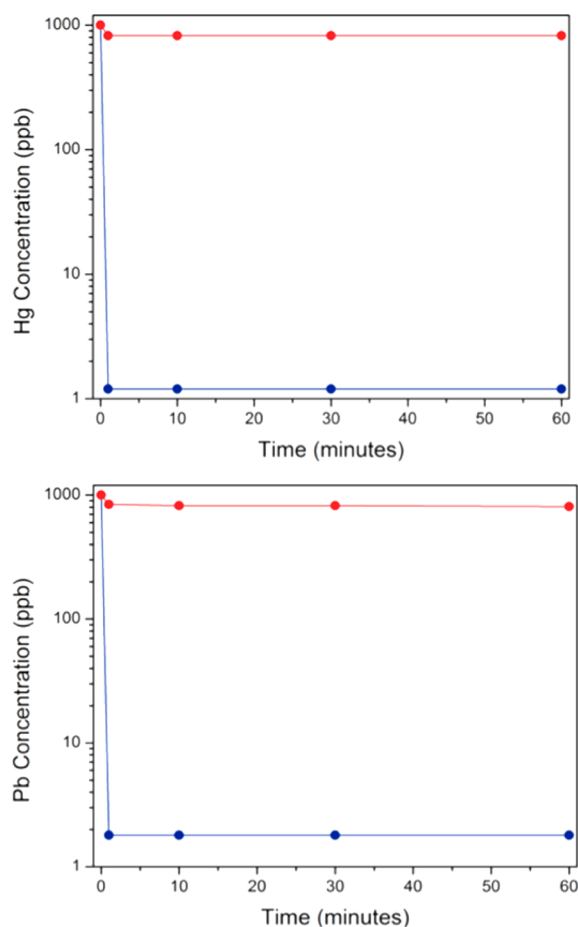

Figure 5. Metal ion concentrations after the treatment of water spiked with 1 ppm of (top) Hg^{2+} and (bottom) Pb^{2+} with Fe-BTC/PDA-19 (blue) or Fe-BTC (red) at different time points.

were treated with the composite, extremely rapid removal and high uptake were recognized. In under a minute, over 99.8% removal of Hg^{2+} and Pb^{2+} is achieved, reducing the concentrations from 1000 to 1.2 and 1.6 ppb, respectively. These values are below the allowable EPA and WHO limits for drinking water. To the best of our knowledge, this composite is the fastest material for the reduction of Hg^{2+} and Pb^{2+} to drinkable concentrations under soaking conditions. The composite achieves impressive uptake capacity without detriment to the fast removal rate observed for the bare Fe-BTC framework. We surmise that this behavior is due to the introduction of extrinsic porosity to the PDA by the MOF template. This phenomenon enhances the heavy metal removal rate and capacity compared to those of the nonporous PDA.[41,42] It should be noted that Ahmed et al. recently reported a nanoselenium sponge that also removes Hg^{2+} in seconds.[43] However, they use 30 times more material, and while the nanoselenium sponge does irreversibly bind mercury

allowing for easy disposal if used for in-home treatment,[44,45] this characteristic might limit its use in wastewater treatment. For Pb^{2+}, the fastest material observed, to date, is a porous polymer, mPMF (mesoporous polymelamine-formaldehyde), that reportedly gets below the EPA limit also in seconds; however, the capacity for this material is extremely low, 0.628 mg of Pb^{2+}/g, requiring large amounts of sorbent to achieve the same performance as Fe-BTC/PDA (Table S4).[46]

Selectivity over common organics or inorganics, such as Ca^{2+}, Mg^{2+}, Na^{+}, and K^{+}, found at high concentrations in wastewater or surface water samples, respectively, is the most important factor when evaluating a porous material for water treatment applications. While ions can compete for binding sites, organics can complex metals in solution or block the pores of the adsorbent entirely compromising capacity and/or removal rate. Given this, Fe-BTC/PDA-19 was first tested in the Rhone River samples spiked with high concentrations of Hg^{2+} and Pb^{2+}, up to 1000 ppm (Figure S15). Fe-BTC/PDA's capacities are either increased (for Hg^{2+}) or well maintained (for Pb^{2+}) in the river water, implying the interferents commonly found in surface waters have a minimal effect on composite performance.

The material's ability to competitively maintain efficiencies and rapid extraction rates at sub ppm levels, more typical of exposure cases, is highly desirable.[6] As such, the Rhone River and Mediterranean Sea water were first spiked with 850 and 1050 ppb of Pb^{2+}, respectively. The concentrations of the ions in the solutions were analyzed before and after treatment with Fe-BTC/PDA-19 (Figure 6). The composite is shown to remove more than 99.7% of Pb^{2+} from the Rhone River water, bringing lead concentrations to 2.2 ppb and within the drinkable regime. For the seawater, the final Pb^{2+} concentrations could not be assessed by ICP-MS due to large amounts of Na^{+}; however, the levels are below the detectable limit of the ICP-OES (10 ppb) and, hence, also within the drinkable regime. Remarkably, within error of the experiment, we see no uptake of any metal ions observed in the two water samples, where concentrations of interferents, such as Na^{+}, are up to 14 000 times the concentration of Pb^{2+} (Figure 6). A similar experiment carried out with 860 ppb of Hg^{2+} in the Rhone River water reveals a final level of 8 ppb, a value only slightly above the level deemed drinkable (<2 ppb), and an excellent removal efficiency of ~99%. It should be noted that all tests performed in Mediterranean Sea water spiked with Hg^{2+} indicate some competitive interference with removal efficiencies slightly reduced to ~90%. Last, the extraction rates of Pb^{2+} and Hg^{2+} were examined between 1 and 60 min in both surface water samples; in all of the cases, the equilibrium is reached in under a minute (Figure S22), implying that the removal rates are not affected by inorganic or organic interferents found in river or seawater samples. To date, we have found no materials in the literature with comparable selectivities or rate for the separation of trace contaminants from the real world water samples.

Compared to surface water samples, wastewater is often comprised of fewer competing ions but significantly higher concentrations of organics. Because these organics can readily complex Pb^{2+} ions in solution, we tested the materials performance in a wastewater sample collected from a treatment plant in Switzerland. Given the minimal amount of lead present in the influent stream, the water was spiked with approximately 700 ppb Pb^{2+}. The composite is able to reduce concentrations to drinkable levels, approximately 2 ppb; however, the extraction rate is slightly slower compared to that of the
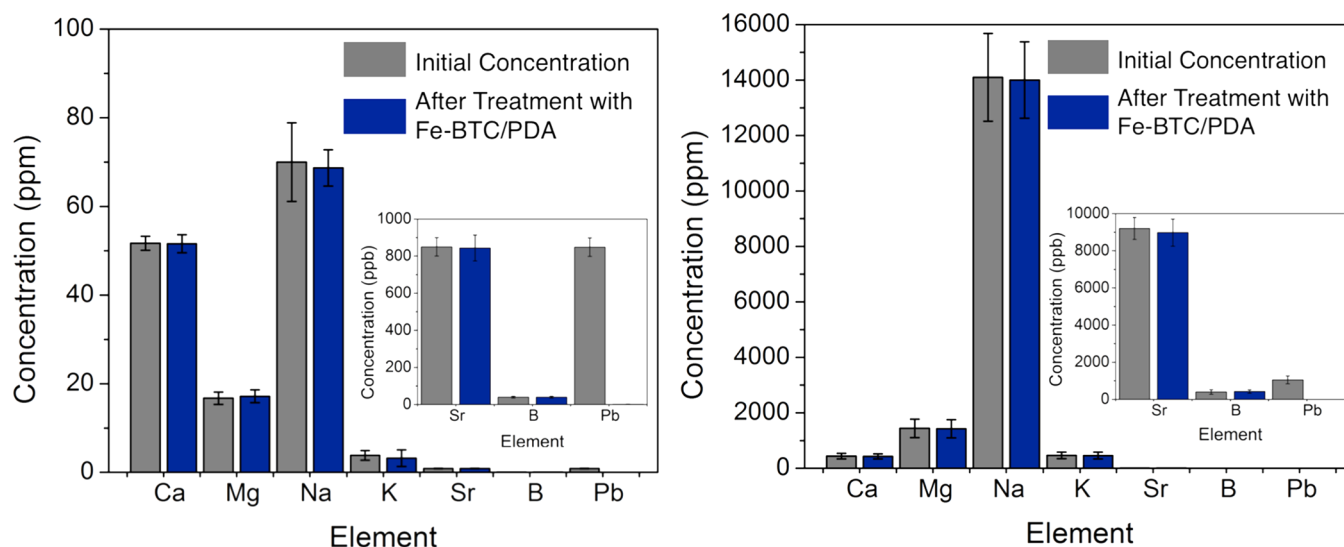
Figure 6. Compositions of the real world samples. (Left) Rhone River water and (right) Mediterranean Sea water were spiked with ∼1 ppm of Pb^{2+} and then subsequently treated with Fe-BTC/PDA-19. The concentrations of ions before and after treatment are denoted as gray and blue, respectively.

surface water samples, which is expected with high levels of lead complexation. Approximately, 70% removal is observed in the first minute, 90% is achieved within the first hour, and up to 99.8% is observed in 24 h. To our knowledge, there are no current studies that evaluate the impact of metal speciation on a material's performance in wastewater, and hence, this is an area we will be required to study for future implementation.

CONCLUDING REMARKS

Fe-BTC/PDA is a novel MOF-polymer composite that has demonstrated the ability to extract large quantities of Pb^{2+} and Hg^{2+} from real world water samples with unprecedented selectivity and rate. The resulting composite promotes the reduction of trace concentrations of Pb^{2+} ions to drinkable levels in under 1 min, even in seawater where interferent concentrations are up to 14 000 times that of Pb^{2+}. These observed properties are derived from introducing extrinsic porosity to an intrinsically nonporous polymer pinned inside of a MOF template. The nanoporous windows of the template not only inhibit leaching of the hydrophilic polymer into the water, enabling easy separation and consistent performance with cycling, but also inhibit the diffusion of large organic interferents into the composite, a phenomenon known to foul most mesoporous adsorbents. Given the demonstrated easy tunability, regeneration, and separation combined with low cost, long-term stability, and high performance in application relevant conditions, this new material could become highly influential for in-home or wastewater treatment technologies, particularly in the event of an impending water crisis. It is envisioned that through judicious selection of MOF and polymer building blocks, this new platform technology could be used to selectively target a wide array of trace contaminants from water and aerial media. Understanding and controlling the properties of highly porous, redox active composites, like Fe-BTC/PDA, will unlock new useful properties for a variety of applications in host–guest chemistry.

ASSOCIATED CONTENT

S Supporting Information

The Supporting Information is available free of charge on the ACS Publications Web site. The Supporting Information is available free of charge on the ACS Publications website at DOI: 10.1021/acscentsci.7b00605.

Materials and methods, additional spectroscopy, electron microscopy, and heavy metal removal data, as well as density functional theory calculations (PDF)

AUTHOR INFORMATION

Corresponding Author

*E-mail: wendy.queen@epfl.ch.

ORCID

Wendy L. Queen: 0000-0002-8375-2341

Notes

The authors declare no competing financial interest.

Kägi for helpful discussions and also for supplying the wastewater samples.

◼ REFERENCES

(1) Gleick, P. H. Global freshwater resources: soft-path solutions for the 21st century. *Science* **2003**, *302*, 1524−1528.

(2) World Health Organization. Drinking-Water Fact-Sheet. http://www.who.int/mediacentre/factsheets/fs391/en/.

(3) WWAP (United Nations World Water Assessment Programme). *Water for a Sustainable World*; The United Nations World Water Development Report: UNESCO:Paris, 2015; pp 1−67.

(4) Tchounwou, P. B.; Yedjou, C. G.; Patlolla, A. K.; Sutton, D. J. Heavy Metals Toxicity and the Environment. *EXS* **2012**, *101*, 133−164.

(5) Shannon, M. A.; Bohn, P. W.; Elimelech, M.; Georgiadis, J. G.; Marinas, B. J.; Mayes, A. M. Science and technology for water purification in the coming decades. *Nature* **2008**, *452*, 301−310.

(6) Sholl, D. S.; Lively, R. P. Seven chemical separations to change the world. *Nature* **2016**, *532*, 435−437.

(7) Ingraham, C. This is how toxic Flint's water really is. https://www.washingtonpost.com/news/wonk/wp/2016/01/15/this-is-how-toxic-flints-water-really-is/.

(8) Pell, M. B.; Schneyer, J. Off the Charts: The thousand of U.S. locales where lead poisoning is worse than Flint. http://www.reuters.com/investigates/special-report/usa-lead-testing/ (accessed 2016).

(9) Luu, T. T. G.; Sthiannopkao, S.; Kim, K.-W. Arsenic and other trace elements contamination in groundwater and a risk assessment study for the residents in the Kandal Province of Cambodia. *Environ. Int.* **2009**, *35* (3), 455−460.

(10) Beaumont, J. J.; Sedman, R. M.; Reynolds, S. D.; Sherman, C. D.; Li, L.-H.; Howd, R. A.; Sandy, M. S.; Zeise, L.; Alexeeff, G. V. Cancer Mortality in a Chinese Population Exposed to Hexavalent Chromium in Drinking Water. *Epidemiology* **2008**, *19* (1), 12−23.

(11) World Health Organization. Lead poisiong and health. http://www.who.int/mediacentre/factsheets/fs379/en/.

(12) Farha, O. K.; Eryazici, I.; Jeong, N. C.; Hauser, B. G.; Wilmer, C. E.; Sarjeant, A. A.; Snurr, R. Q.; Nguyen, S. T.; Yazaydın, A. Ö.; Hupp, J. T. Metal−Organic Framework Materials with Ultrahigh Surface Areas: Is the Sky the Limit? *J. Am. Chem. Soc.* **2012**, *134* (36), 15016−15021.

(13) Furukawa, H.; Cordova, K. E.; O'Keeffe, M.; Yaghi, O. M. The Chemistry and Applications of Metal-Organic Frameworks. *Science* **2013**, *341* (6149), 1230444.

(14) Wang, C.; Liu, X.; Keser Demir, N.; Chen, J. P.; Li, K. Applications of water stable metal-organic frameworks. *Chem. Soc. Rev.* **2016**, *45* (18), 5107−5134.

(15) Demessence, A.; D'Alessandro, D. M.; Foo, M. L.; Long, J. R. Strong CO2 Binding in a Water-Stable, Triazolate-Bridged Metal−Organic Framework Functionalized with Ethylenediamine. *J. Am. Chem. Soc.* **2009**, *131* (25), 8784−8786.

(16) McDonald, T. M.; Mason, J. A.; Kong, X.; Bloch, E. D.; Gygi, D.; Dani, A.; Crocella, V.; Giordanino, F.; Odoh, S. O.; Drisdell, W. S.; Vlaisavljevich, B.; Dzubak, A. L.; Poloni, R.; Schnell, S. K.; Planas, N.; Lee, K.; Pascal, T.; Wan, L. F.; Prendergast, D.; Neaton, J. B.; Smit, B.; Kortright, J. B.; Gagliardi, L.; Bordiga, S.; Reimer, J. A.; Long, J. R. Cooperative insertion of CO2 in diamine-appended metal-organic frameworks. *Nature* **2015**, *519* (7543), 303−308.

(17) Uemura, T.; Yanai, N.; Kitagawa, S. Polymerization reactions in porous coordination polymers. *Chem. Soc. Rev.* **2009**, *38* (5), 1228−1236.

(18) Alsbaiee, A.; Smith, B. J.; Xiao, L.; Ling, Y.; Helbling, D. E.; Dichtel, W. R. Rapid removal of organic micropollutants from water by a porous *β*-cyclodextrin polymer. *Nature* **2016**, *529* (7585), 190−194.

(19) Li, B.; Zhang, Y.; Ma, D.; Shi, Z.; Ma, S. Mercury nano-trap for effective and efficient removal of mercury(II) from aqueous solution. *Nat. Commun.* **2014**, *5*, 5537−5543.

(20) Knight, A. S.; Zhou, E. Y.; Pelton, J. G.; Francis, M. B. Selective Chromium(VI) Ligands Identified Using Combinatorial Peptoid Libraries. *J. Am. Chem. Soc.* **2013**, *135* (46), 17488−17493.

(21) Horcajada, P.; Chalati, T.; Serre, C.; Gillet, B.; Sebrie, C.; Baati, T.; Eubank, J. F.; Heurtaux, D.; Clayette, P.; Kreuz, C.; Chang, J.-S.; Hwang, Y. K.; Marsaud, V.; Bories, P.-N.; Cynober, L.; Gil, S.; Ferey, G.; Couvreur, P.; Gref, R. Porous metal-organic-framework nanoscale carriers as a potential platform for drug delivery and imaging. *Nat. Mater.* **2010**, *9* (2), 172−178.

(22) Férey, G.; Serre, C.; Mellot-Draznieks, C.; Millange, F.; Surblé, S.; Dutour, J.; Margiolaki, I. A Hybrid Solid with Giant Pores Prepared by a Combination of Targeted Chemistry, Simulation, and Powder Diffraction. *Angew. Chem., Int. Ed.* **2004**, *43* (46), 6296−6301.

(23) Horcajada, P.; Surble, S.; Serre, C.; Hong, D.-Y.; Seo, Y.-K.; Chang, J.-S.; Greneche, J.-M.; Margiolaki, I.; Ferey, G. Synthesis and catalytic properties of MIL-100(Fe), an iron(iii) carboxylate with large pores. *Chem. Commun.* **2007**, *27*, 2820−2822.

(24) Lee, H.; Dellatore, S. M.; Miller, W. M.; Messersmith, P. B. Mussel-Inspired Surface Chemistry for Multifunctional Coatings. *Science* **2007**, *318* (5849), 426−430.

(25) Seo, Y.-K.; Yoon, J. W.; Lee, J. S.; Lee, U. H.; Hwang, Y. K.; Jun, C.-H.; Horcajada, P.; Serre, C.; Chang, J.-S. Large scale fluorine-free synthesis of hierarchically porous iron(III) trimesate MIL-100(Fe) with a zeolite MTN topology. *Microporous Mesoporous Mater.* **2012**, *157*, 137−145.

(26) Dhakshinamoorthy, A.; Alvaro, M.; Horcajada, P.; Gibson, E.; Vishnuvarthan, M.; Vimont, A.; Grenèche, J.-M.; Serre, C.; Daturi, M.; Garcia, H. Comparison of Porous Iron Trimesates Basolite F300 and MIL-100(Fe) As Heterogeneous Catalysts for Lewis Acid and Oxidation Reactions: Roles of Structural Defects and Stability. *ACS Catal.* **2012**, *2* (10), 2060−2065.

(27) El-Ayaan, U.; Herlinger, E.; Jameson, R. F.; Linert, W. Anaerobic oxidation of dopamine by iron(III). *J. Chem. Soc., Dalton Trans.* **1997**, *16*, 2813−2818.

(28) Zangmeister, R. A.; Morris, T. A.; Tarlov, M. J. Characterization of Polydopamine Thin Films Deposited at Short Times by Autoxidation of Dopamine. *Langmuir* **2013**, *29* (27), 8619−8628.

(29) Liu, Y.; Ai, K.; Lu, L. Polydopamine and Its Derivative Materials: Synthesis and Promising Applications in Energy, Environmental, and Biomedical Fields. *Chem. Rev.* **2014**, *114* (9), 5057−5115.

(30) Ang, J. M.; Du, Y.; Tay, B. Y.; Zhao, C.; Kong, J.; Stubbs, L. P.; Lu, X. One-Pot Synthesis of Fe(III)−Polydopamine Complex Nanospheres: Morphological Evolution, Mechanism, and Application of the Carbonized Hybrid Nanospheres in Catalysis and Zn−Air Battery. *Langmuir* **2016**, *32* (36), 9265−9275.

(31) Sever, M. J.; Weisser, J. T.; Monahan, J.; Srinivasan, S.; Wilker, J. J. Metal-Mediated Cross-Linking in the Generation of a Marine-Mussel Adhesive. *Angew. Chem., Int. Ed.* **2004**, *43* (4), 448−450.

(32) Guo, Z.; Ni, K.; Wei, D.; Ren, Y. Fe3+-induced oxidation and coordination cross-linking in catechol-chitosan hydrogels under acidic pH conditions. *RSC Adv.* **2015**, *5* (47), 37377−37384.

(33) *2012 ed. of the Drinking Water Standards and Health Advisories*; U.S. Environmental Protection Agency, 2012.

(34) Li, B.; Zhang, Z.; Li, Y.; Yao, K.; Zhu, Y.; Deng, Z.; Yang, F.; Zhou, X.; Li, G.; Wu, H.; Nijem, N.; Chabal, Y. J.; Lai, Z.; Han, Y.; Shi, Z.; Feng, S.; Li, J. Enhanced Binding Affinity, Remarkable Selectivity, and High Capacity of CO$_2$ by Dual Functionalization of a rht-Type Metal-Organic Framework. *Angew. Chem., Int. Ed.* **2012**, *51* (6), 1412−1415.

(35) Mon, M.; Lloret, F.; Ferrando-Soria, J.; Martí-Gastaldo, C.; Armentano, D.; Pardo, E. Selective and Efficient Removal of Mercury from Aqueous Media with the Highly Flexible Arms of a BioMOF. *Angew. Chem., Int. Ed.* **2016**, *55* (37), 11167−11172.

(36) Meri-Bofi, L.; Royuela, S.; Zamora, F.; Ruiz-Gonzalez, M. L.; Segura, J. L.; Munoz-Olivas, R.; Mancheno, M. J. Thiol grafted imine-based covalent organic frameworks for water remediation through selective removal of Hg(ii). *J. Mater. Chem. A* **2017**, *5* (34), 17973−17981.

(37) Yu, C.; Shao, Z.; Hou, H. A functionalized metal-organic framework decorated with O- groups showing excellent performance for lead(ii) removal from aqueous solution. *Chem. Sci.* **2017**, *8*, 7611−7619.

(38) Asiabi, H.; Yamini, Y.; Shamsayei, M.; Tahmasebi, E. Highly selective and efficient removal and extraction of heavy metals by layered double hydroxides intercalated with the diphenylamine-4-sulfonate: A comparative study. *Chem. Eng. J.* **2017**, *323*, 212−223.

(39) Tang, W.-W.; Zeng, G.-M.; Gong, J.-L.; Liang, J.; Xu, P.; Zhang, C.; Huang, B.-B. Impact of humic/fulvic acid on the removal of heavy metals from aqueous solutions using nanomaterials: A review. *Sci. Total Environ.* **2014**, *468−469*, 1014−1027.

(40) Terdkiatburana, T.; Wang, S.; Tadé, M. O. Competition and complexation of heavy metal ions and humic acid on zeolitic MCM-22 and activated carbon. *Chem. Eng. J.* **2008**, *139* (3), 437−444.

(41) Zhang, X.; Jia, X.; Zhang, G.; Hu, J.; Sheng, W.; Ma, Z.; Lu, J.; Liu, Z. Efficient removal and highly selective adsorption of Hg2+ by polydopamine nanospheres with total recycle capacity. *Appl. Surf. Sci.* **2014**, *314*, 166−173.

(42) Lee, M.; Rho, J.; Lee, D.-E.; Hong, S.; Choi, S.-J.; Messersmith, P. B.; Lee, H. Water Detoxification by a Substrate- Bound Catecholamine Adsorbent. *ChemPlusChem* **2012**, *77* (11), 987−990.

(43) Ahmed, S.; Brockgreitens, J.; Xu, K.; Abbas, A. A Nanoselenium Sponge for Instantaneous Mercury Removal to Undetectable Levels. *Adv. Funct. Mater.* **2017**, *27* (17), 1606572.

(44) U.S. EPA Method 1311: Toxicity Characteristic Leaching Procedure 1992. https://www.epa.gov/sites/production/files/2015-12/documents/1311.pdf.

(45) U.S. EPA Method 1312: Synthetic Precipitation Leaching Procedure 1994. https://www.epa.gov/sites/production/files/2015-12/documents/1312.pdf.

(46) Tan, M. X.; Sum, Y. N.; Ying, J. Y.; Zhang, Y. A mesoporous poly-melamine-formaldehyde polymer as a solid sorbent for toxic metal removal. *Energy Environ. Sci.* **2013**, *6* (11), 3254−3259.